Quadrature Mismatch Shaping with a Complex, Data Directed Swapper.

Stijn Reekmans, Benoit Catteau, Pieter Rombouts and Ludo Weyten

Department of Electronics and Information Systems (ELIS), Ghent University (UGent)
Sint-Pietersnieuwstraat 41, 9000 Ghent, Belgium (e-mail: Stijn.Reekmans@ELIS.UGent.be)

***Abstract*— Quadrature bandpass (QBP) $\Sigma\Delta$ ADCs require a feedback path for both the I and the Q part of the complex feedback signal. A complex DAC could give this feedback with near-perfect I/Q balance. Still, the mismatch between the unit elements of the complex DAC introduces mismatch noise that should be shaped out of the signal band with dynamic element-matching (DEM) techniques. To select the unit DAC elements of the complex multibit DAC, the well-known data directed swapper is generalized towards a complex structure and the necessary constraints for its correct functioning are derived. Additionally, a hardware efficient structure is presented: the reduced butterfly shuffler. Here, some of the QBP swapper cells are replaced by bandpass (BP) swapper cells. Also, great attention is paid to the interconnection pattern of the data directed swapper to prevent instability.**

I. Introduction

In low-IF receivers, quadrature bandpass (QBP) $\Sigma\Delta$ modulators provide interesting advantages over a pair of real bandpass $\Sigma\Delta$ modulators [1]. Such a QBP $\Sigma\Delta$ modulator takes in a complex analog input and produces a complex digital output which represents the complex input within a narrow bandwidth. As such, it performs complex analog-to-digital conversion. Complex signals are a convenient representation of a pair of real signals. One signal is interpreted as the real part (indicated with sub- or superscript I) and the other signal as the imaginary part (indicated with sub- or superscript Q) of the combined complex signal [2].

Whereas traditional $\Sigma\Delta$ modulators employed 1-bit quantization, multibit $\Sigma\Delta$ ADCs achieve a higher resolution and alleviate stability problems [3]. However, multibit DACs are not inherently linear since they suffer from mismatch between the DAC elements. Furthermore, most of the QBP $\Sigma\Delta$ modulators are using two separate feedback DACs, one real DAC for the feedback of the in-phase (I) path, another one for the quadrature (Q) path. For this combination, the mismatch results in a non-linear error, called DAC mismatch noise, and in path mismatch between the I- and Q-path. This path mismatch causes both the input signal and the quantization noise in the image band to fold into the desired signal band. For QBP modulators this is highly unwanted since quantization noise is not attenuated in the image band [4], [5].

An interesting approach, to solve the mismatch between the paths, is to merge the two real DACs into one complex multibit DAC structure [5], [6]. The architecture of such a complex multibit DAC is shown in Fig. 1. Next to a DAC bank consisting of N unit elements, it contains an element selection logic block (ESL). The task of the ESL is to map each complex input sample $x[n]$ to complex selection signals $x_i[n]$ such that the sum of the N selection signals equals $x[n]$. Each of the N unit elements can be selected in three ways. If the selection signal $x_i = 1$, the unit element is selected 'I' and gives feedback to the I-path. When $x_i = j$, the unit element is selected 'Q' and gives feedback to the Q-path and when $x_i = 0$, the unit element is unselected and generates no feedback.

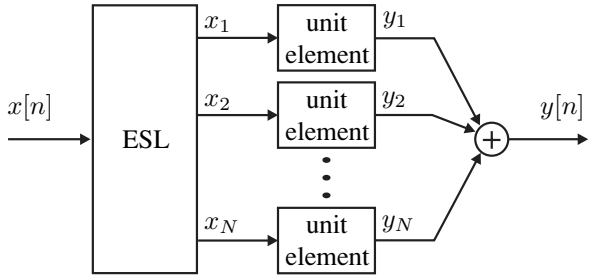

Fig. 1. A complex multibit DAC with ESL.

Since all the unit elements in a complex DAC belong to a common pool, it is possible to process the I and Q signals in exactly the same way. As a result, the difference between the I- and Q-path disappears and the problem related to path mismatch can be solved. Still, the mismatch between the unit elements of the complex DAC introduces mismatch noise. It should be guaranteed that the power of this error is shaped out of the signal band with dynamic element-matching (DEM) techniques.

Thus far, DEM schemes based on the data directed swapper are used to whiten [7] or to lowpass shape [8] the mismatch errors. [9] shows how the data directed swapper can be endowed with arbitrary real mismatch shaping characteristics. Recently, a more accurate technique to obtain a second order bandpass shaping with the data directed swapper was introduced [10]. All these structures are only applicable for real DAC structures. In the next section it is shown how the well-known data directed swapper can be generalized towards a complex structure. This new structure allows QBP shaping of the DAC noise. As such, it forms an alternative for the complex tree structured DAC of [5].

1-4244-0395-2/06/$20.00 ©2006 IEEE.

II. A Complex, Data Directed Swapper

A. Architecture

The complex data directed DAC consists of a digital encoder, a data directed ESL and a unit DAC bank. In Fig. 2, a DAC architecture with 4 (b=2) unit elements is shown to illustrate the principle. The complex data directed ESL requires that its N=2^b input signals are limited to $\{0, 1, j\}$. However, since the input of the complex data directed DAC $x[n]$ is interpreted as a complex integer, $x[n] \in \{x_I[n] + jx_Q[n] : 0 \leq x_I[n], x_Q[n] \leq 2^{b-1}\}$, a digital encoder is necessary to encode the complex integer $x[n]$ into the three-level format. This is the task of the digital encoder in Fig. 2. It will decompose each complex input sample $x[n]$ into four three-level signals $(x_{2,1}[n], ..., x_{2,4}[n])$ such that its sum equals $x[n]$. This decomposition is memoryless and time invariant.

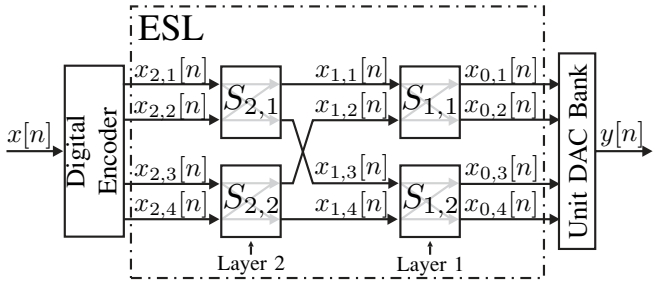

Fig. 2. Complex data directed DAC with a four element unit DAC bank.

The complex data directed ESL itself consists of a (bxb) matrix of swapper cells $S_{k,r}$, where k and r denote the layer number and the position within the layer respectively. Each swapper cell has two inputs $x_{k,2r-1}$ and $x_{k,2r}$ and two outputs which are connected to two different swapper cells of layer k-1. At each sample time n, each swapper cell determines its outputs by routing its inputs either straight through or crossed. This way, the ESL will dynamically assign every input signal of the ESL to one of the output signals $x_{0,i}[n]$.

The behavior of the swapper cell is based on the swapper sequence $s_{k,r}$. This sequence is defined as the difference between the two outputs. To illustrate this, the input/output relationship of swapper cell $S_{1,1}$ is given by:

$$\begin{aligned} x_{0,1}[n] &= \tfrac{1}{2}(x_{1,1}[n] + x_{1,2}[n] + s_{1,1}[n]) \\ x_{0,2}[n] &= \tfrac{1}{2}(x_{1,1}[n] + x_{1,2}[n] - s_{1,1}[n]) \end{aligned} \quad (1)$$

As shown in [3], [11], the DAC mismatch error is a linear combination of the swapper sequences. So, if each swapper sequence is calculated as a K^{th} order shaped sequence that is uncorrelated with the sequences of the other swapper cells, then the DAC error will be a K^{th} order shaped sequence.

These swapper sequences need to fulfill the following constraints:

$$s_{k,r}[n] = \begin{cases} 0 & \text{if } x_{k,2r\text{-}1}[n]{+}x_{k,2r}[n] \text{ is 0, 2 or } 2j \\ \pm 1 & \text{if } x_{k,2r\text{-}1}[n]{+}x_{k,2r}[n] \text{ is 1} \\ \pm j & \text{if } x_{k,2r\text{-}1}[n]{+}x_{k,2r}[n] \text{ is } j \\ \pm 1 \mp j & \text{if } x_{k,2r\text{-}1}[n]{+}x_{k,2r}[n] \text{ is 1+}j \end{cases} \quad (2)$$

to ensure that the real and imaginary part of the outputs of the swapper cells are natural numbers after the division by two in eq. (1) and that the output of these cells is restricted to $\{0, 1, j\}$.

B. QBP Shaper

The QBP shaper will calculate the swapper sequence as a QBP shaped sequence. Essentially, the QBP shaper consists of a digital domain QBP $\Sigma\Delta$ modulator with no input signal, where the two quantizers are replaced by one restricted quantizer (see Fig. 3). The restricted quantizer tries to follow its inputs $(sv^I_{k,r}[n], sv^Q_{k,r}[n])$ while forcing its outputs $(s^I_{k,r}[n], s^Q_{k,r}[n])$ to fulfill the constraints of eq.(2).

The restricted quantizer can be modelled as an additive error $\mathrm{L}(z) = \mathrm{L}_I + j\mathrm{L}_Q$, leading to the linear model of Fig. 3 on the right. The complex loopfilter $\mathrm{H}(z)$ ensures that this additive error is shaped. With $S_{k,r}(z)$ denoting the $\mathcal{Z}$-transform of the switching sequence and $\mathrm{MTF}(z)$ the complex mismatch transfer function, we have:

$$S_{k,r}(z) = \frac{1}{1 + \mathrm{H}(z)}\mathrm{L}(z) = \mathrm{MTF}(z)\mathrm{L}(z) \quad (3)$$

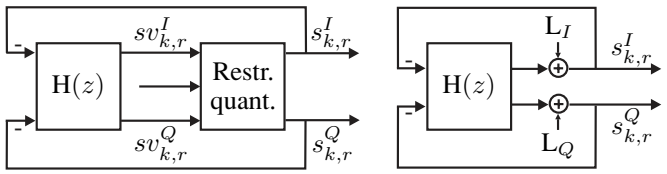

Fig. 3. QBP shaper and its linear model.

In general, the output $s^I_{k,r}[n]$ (resp. $s^Q_{k,r}[n]$) has the sign of its state variable $sv^I_{k,r}[n]$ (resp. $sv^Q_{k,r}[n]$) or equals zero in case $x^I_{k,2r\text{-}1}[n]{+}x^I_{k,2r}[n]$ (resp. $x^Q_{k,2r\text{-}1}[n]{+}x^Q_{k,2r}[n]$) is even. However, two special cases can occur:

1) In case of a zero state variable, its sign is indefinite and the sign of the output can be chosen (e.g. alternately) if the input is odd.

2) If both real and imaginary parts are odd, a contention can appear if both state variables have the same sign. In this case, the state variable with the largest absolute value is given preferential treatment. This means that this state variable will decide the sign of its corresponding output. The other output will then have the opposite sign. If both state variables are equal, we could chose to give preferential treatment to the I-path. However, the I- and Q-path of the complex DAC are now not treated in the same way, resulting in path mismatch. Therefore, we suggest to toggle between the preferential treatment of the two paths so that, on average, neither the I- or the Q-path is preferred. As a result, the I and Q signals are treated in exactly the same way and will not suffer from path mismatch.

C. Thermometer Encoder and Interconnection

A possible implementation of the digital encoder of Fig. 2, which encodes the complex integer $x[n]$ into the correct three-level format $\{0, 1, j\}$, is a combination of two thermometer

encoders. One thermometer encoder is used for the I-path, the other one for the Q-path, see Fig. 4. This digital encoder follows the transformation equations:

$$x_i[n] = \begin{cases} 1 & \text{if } i \leq x^I[n] \\ 0 & \text{otherwise} \end{cases} \tag{4}$$

for $1 \leq i \leq N/2$ and:

$$x_i[n] = \begin{cases} j & \text{if } N - i < x^Q[n] \\ 0 & \text{otherwise} \end{cases} \tag{5}$$

for $N/2+1 \leq i \leq N$. This is also illustrated at the very right of Fig. 4.

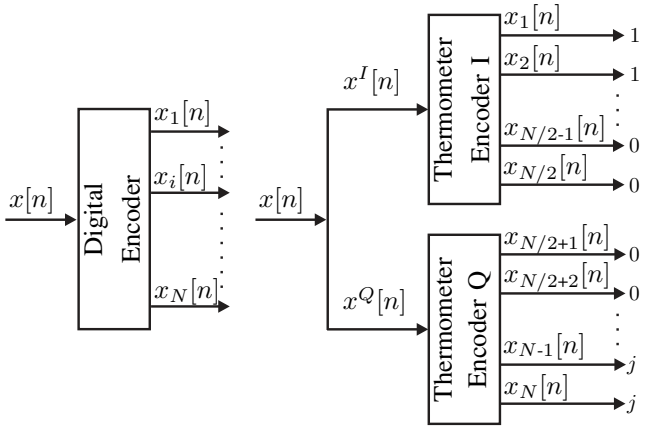

Fig. 4. Complex digital encoder with two real thermometer encoders.

Concerning the interconnection of the digital encoder with the data directed ESL, it should be avoided that any QBP swapper cell has strictly real or strictly imaginary inputs. Suppose that the sequence $x^I_{k,2r\text{-}1}[n]$+$x^I_{k,2r}[n]$ is strictly real for every sample time n, then $s^Q_{k,r}[n]$ equals zero due to the constraints in the restricted quantizer (eq. (2)). In this case, the model for the restricted quantizer as two additive error terms is not justified. Indeed, since $s^Q_{k,r}[n]$ equals zero all the time, the quadrature feedback path disappears, as shown in Fig. 5. The same conclusion can be drawn for a strictly imaginary valued sequence $x^I_{k,2r\text{-}1}[n]$+$x^I_{k,2r}[n]$.

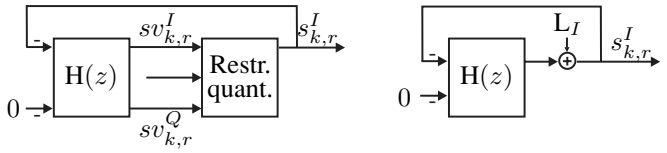

Fig. 5. QBP shaper and its linear model in case of a strictly real valued sequence $x^I_{k,2r\text{-}1}[n]$+$x^I_{k,2r}[n]$.

In the situation of Fig. 5, the shaping of the $s_{k,r}[n]$ sequence will deviate from eq. (3):

$$S_{k,r}(z) = \frac{1}{1 + \mathrm{H}'(z)} \mathrm{L}_I(z) = \mathrm{MTF}'(z)\mathrm{L}_I(z) \tag{6}$$

Here, $\mathrm{H}'(z)$ is the $\mathcal{Z}$-transform of the real part of $h[n]$:

$$\mathrm{H}'(z) = \frac{\mathrm{H}(z) + \mathrm{H}^*(z^*)}{2} \tag{7}$$

Obviously $\mathrm{MTF}'(z)$ deviates from $\mathrm{MTF}(z)$, which may lead to unexpected behaviour. We have verified that for first order QBP shaping, good performance is still ensured since the QBP shaping is altered into a BP shaping with similar properties. This way first order QBP mismatch shaping is guaranteed to be "fail-safe". However, it was found that instability can occur for higher order QBP mismatch shaping. In this case, it is important to prevent this situation. Fortunately, this is easily achieved by appropriately choosing the interconnection pattern.

Fig. 6 show such an appropriate interconnection pattern. Here, the outputs of the thermometer encoder I and Q are cross-coupled, so that every swapper cell has a complex input.

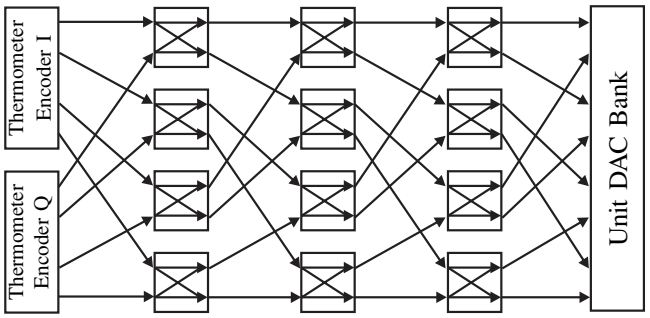

Fig. 6. Complex data directed DAC.

D. Reduced QBP Shaped Data Directed DAC

In Fig. 7, an alternative interconnection pattern is shown. In this ESL topology, we have opted for keeping the I- and Q-path separated as long as possible (marked with the dash dot line). Only in the last layer, there is a coupling between the I- and Q-path. Note that now the input of the QBP cells are strictly real or imaginary. This way the QBP shaped swapper cells of all but the last layer should be replaced by real BP shaped swapper cells such as those presented in [10].

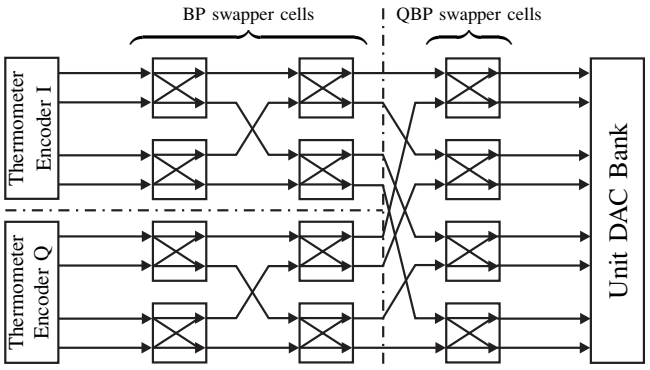

Fig. 7. Reduced QBP data directed DAC.

The replacement of QBP- into BP shaped swapper cells results in a more hardware efficient implementation since real BP shaped swapper cells use less hardware than complex QBP shaped swapper cells. In order to get a first idea of the hardware reduction, we performed actual digital gate-level synthesis of the required hardware of both structures. This

design experiment reveals that in most cases, the hardware complexity is almost reduced by a factor of two.

III. Simulation Results

To illustrate the effectiveness of the proposed approach, extensive simulations, for the case of first order $f_s/4$ mismatch shaping, were performed. As a test structure, a complex DAC, with the presented reduced data directed swapper was employed. The same first order $f_s/4$ QBP loopfilter as in [5] was used to obtain the swapper sequences. The DAC was placed in the feedback path of a typical discrete time $\Sigma\Delta$ modulator. A fourth order NTF(z) was used with an H_∞=1.5 and a center frequency f_c=0.25. The complex DAC bank contains 8 unit DAC elements which were assigned a zero-mean random mismatch with a standard deviation σ of 1%. The $\Sigma\Delta$ modulator was stimulated with two different complex input signals. One is situated in the in-band region at f=0.2501, the other one in the mirror band at f=0.7502. The amplitude of both signals is -6dB of full scale.

In Fig. 8, the DAC mismatch error spectrum is shown for the case one of the paths gets preferential treatment when there is a choice in the restricted quantizer. We notice that there is some signal feedthrough and signals in the image band that alias into the desired signal band and vice versa. This folding is the result of the fact that the I- and Q-path of the complex DAC are not treated in the same way.

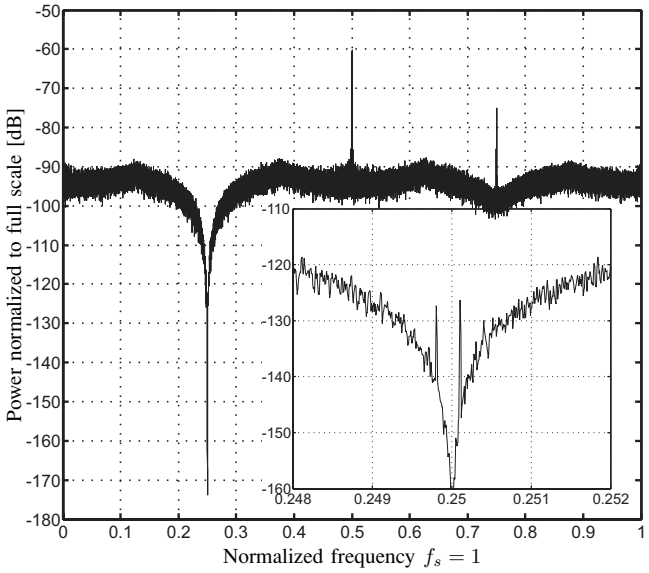

Fig. 8. DAC error spectrum in case one of the paths of the reduced data directed swapper gets preferential treatment (12 times averaged 128K FFT).

In Fig. 9, the DAC mismatch error spectrum is shown for the case the I- and Q-path of the complex DAC are treated in the same way by toggling between the preferential treatment of the two paths so that, on average, neither the I- or the Q-path is preferred. Here no folding of the signals occurs.

The DAC error spectra in case of the data directed swapper are omitted due to place limitation, but the same conclusion as for the reduced data directed swapper could be drawn.

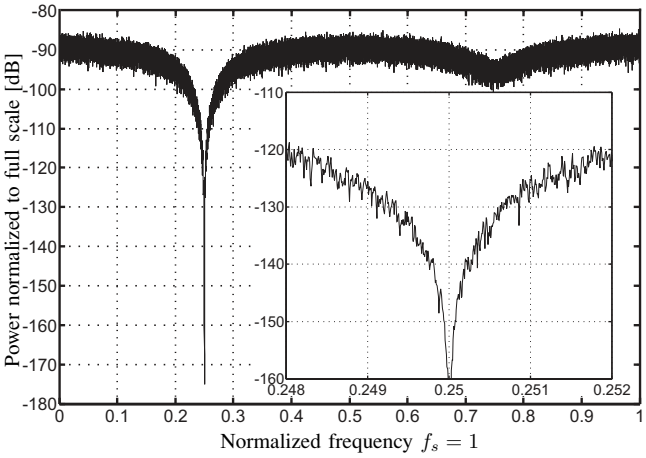

Fig. 9. DAC error spectrum in case the paths of the reduced data directed swapper are treated in the same way (12 times averaged 128K FFT).

IV. Conclusion

Realizing the feedback structure of the multibit QBP $\Sigma\Delta$ ADC with one complex multibit DAC has the advantage that path mismatch disappears in contrast to a realization with two separate real multibit DAC structures. In this work, we have shown how the real data directed swapper can be adapted toward a quadrature bandpass structure. We have shown that it should be avoided that any QBP swapper cell has strictly real or strictly imaginary inputs. Additionally, we presented a novel structure with lower hardware complexity, i.e. the reduced data directed swapper. Here, some of the quadrature bandpass cells are replaced by more hardware efficient bandpass cells.

Acknowledgement

S. Reekmans and B. Catteau are supported by the Special Research Fund of Ghent University.

References

[1] S. Jantzi, K. Martin, and A. Sedra, "Quadrature Bandpass $\Delta\Sigma$ Modulation for Digital Radio," *IEEE J. Solid-State Circuits*, vol. 32, no. 12, 1997.

[2] K. W. Martin, "Complex Signal Processing is Not Complex," *IEEE Trans. Circuit Syst. I*, vol. 51, no. 9, 2004.

[3] I. Galton, "Spectral Shaping of Circuit Errors in Digital-to-Analog Converters," *IEEE Trans. Circuits Syst. II*, vol. 44, no. 10, 1997.

[4] R. Maurino and C. Papavassiliou, "Multibit Quadrature Sigma-Delta Modulator with DEM Scheme," *IEEE International Symposium on Circuits and Systems, ISCAS*, 2004.

[5] S. Reekmans, J. De Maeyer, P. Rombouts, and L. Weyten, "Quadrature Mismatch Shaping with a Complex, Tree Structured DAC," *IEEE International Symposium on Circuits and Systems, ISCAS*, 2006.

[6] R. Schreier, "Quadrature Mismatch-Shaping," *IEEE International Symposium on Circuits and Systems, ISCAS*, 2002.

[7] L. R. Carley, "A Noise-shaping Coder Topology for 15+ bit Converters," *IEEE J. Solid-State Circuits*, vol. 24, no. 2, 1989.

[8] R. W. Adams and T. W. Kwan, "Data-directed Scrambler for Multi-bit Noiseshaping D/A Converters," *U.S. Patent Number 5404142*, 1995.

[9] H. Lin and R. Schreier, "A Bandpass Mismatch-Shaped Multi-Bit $\Sigma\Delta$ Switched-Capacitor DAC using Butterfly Shuffler."

[10] M. Vadipour, "A Bandpass Mismatch Noise-Shaping Technique for $\Sigma\Delta$ Modulators," *IEEE Trans. Circuits Syst. II, Express Briefs.*, vol. 51, no. 3, pp. 130–135, 2004.

[11] J. Welz and I. Galton, "Necessary and Sufficient Conditions for Mismatch Shaping in a General Class of Multibit DACs," *IEEE Trans. Circuits Syst. II*, vol. 49, no. 12, pp. 748–759, 2002.